2244

Electro-optically controlled beam switching via total internal reflection at a domain-engineered interface in $LiNbO_3$

Alexander J Boyland*, Sakellaris Mailis, Jason M Hendricks, Peter G R Smith, Robert W Eason.

Optoelectronics Research Centre

University of Southampton

Southampton

SO17 1BJ

UK.

* corresponding author

Tel 023 80594527: Fax 023 80593142 : e-mail **ajb@orc.soton.ac.uk**

Submitted to Opt. Commun

May 2001.

Key words : total internal reflection, switching, electro-optic effect, Lithium Niobate, grazing incidence, domain-engineering

Abstract

We report a novel switching method that occurs due to the electro-optic effect under applied field when a beam incident on an interface between anti-parallel domains in a sample of $LiNbO_3$ subtends an angle greater than that required for total internal reflection (TIR). We present data obtained for wavelengths of 0.543 μm and 1.52 μm and compare this with a theoretical model. This switch has many attractive properties, as TIR is a 100% efficient process leading to the possibility of high contrast ratios; current data shows contrast ratios greater than 100:1 (20dB). Other properties include relatively simple fabrication procedure, low drive voltages and a wavelength dependence that is less than other electro-optic devices such as Pockels cells.

1. Introduction

We have developed a novel switching technique [1] that uses the electro-optic effect to induce a change in the refractive index, Δn, of a material that has been domain-engineered to produce a boundary between two anti-parallel domain regions. When a beam is incident on the interface between these oppositely oriented domains at a suitably large angle, total internal reflection (TIR) can occur for a sufficiently large difference in refractive indices electrically induced between the two anti-parallel domains.

This method of electro-optically induced TIR is a novel approach for achieving high contrast switching, and presents many advantages when compared to existing techniques that use electro-optic deflection across a boundary [2] rather than reflection at an interface. The values of induced Δn are typically low for electro-optically addressed interfaces between domain engineered $LiNbO_3$, so prism-type scanning devices have inherently low angular deflection sensitivity. For grazing incidence geometries however, TIR can be extremely sensitive, and for sufficiently large angles of incidence approaching 90^o, the voltages required to induce switching can be of order a few volts.

To our knowledge such electro-optic TIR switching has not been reported before for domain-engineered ferroelectric hosts. A paper reporting electro-optic deflection across the interface describes our work in large angle (up to 10^o) scanning [3], but this work is different, and does not consider the stage of actual TIR switching.

2. Background

The angle necessary for TIR at an electro-optically addressed interface is given by the usual expression below;

$$\sin\theta_{tir} = \frac{n - \Delta n}{n + \Delta n} \tag{1}$$

where the equation relating Δn, and electric field, E, is given by the usual expression below

$$\Delta n = -\frac{1}{2} r_{33} n_e^3 E_z \tag{2}$$

where r_{33} is the largest electro-optic coefficient accessed by extraordinary s-polarised light, n_e is the wavelength dependent value of extraordinary refractive index, and E_z is the value of electric field applied across the sample in the z-direction. While these coefficients which relate to s-polarised light lead to better switching characteristics, switching will also occur when using ordinary p-polarised light, that accesses the r_{13} electro-optic coefficient which has a value approximately 1/3 that of r_{33}, and n_e is replaced by n_o, the value of the ordinary refractive index.

The value used for r_{33} was 30.8 x 10^{-12} mV^{-1}[4] which was the closest published value corresponding to 0.543μm and the value for n_e was 2.23 [4] evaluated from the Sellmeier equation for a wavelength of 0.543 μm.

Table 1 below shows values of Δn produced and the angle (θ_{tir}) necessary for TIR for increasing values of applied voltage for a 300 μm thick sample, where Δn^* is double the value of Δn calculated from (2) as the change in value of refractive index on each side of the interface is of opposite sign. Fig 1 shows the minimum angle required for switching to occur as a function of applied voltage.

3. Switch experimental details

The schematic of the electro-optically controllable domain engineered TIR switch can be seen in fig 2. The sample was a z-cut wafer of congruent $LiNbO_3$ supplied by Yamaju (Japan), of thickness 300μm, and dimensions 13.5 mm x 15mm in the x and y directions respectively. The two anti-parallel domains were produced by firstly photolithographically patterning the –z face and then electric field poling the sample. When examined under a polarising optical microscope the interface was seen to be quite smooth, but under high magnification some variation from absolute straightness was observed. This can be seen in fig 3, which shows an example of a region of such deviation from linearity. This non-uniformity was observed for all the samples but its extent was dependent on the poling parameters used, and also varied between individual samples. The samples were annealed after poling to assist the removal of any residual strain at the interface. Even after annealing for several hours at 200°C however, a small residual refractive index of order 10^{-5} existed at the interface [1]. This residual refractive index can lead to significant Fresnel reflections at grazing angle incidence which will in turn affect the choice of incidence angle used and therefore the contrast ratio achievable.

Experimental data was obtained using polarised He-Ne lasers at wavelengths of 0.543μm and 1.52μm. In each case the beam was initially passed through a spatial filter consisting of two microscope objectives (x10) and a pinhole before being focussed into the $LiNbO_3$ sample. Focussing was achieved using a lens of focal length 160mm, which produced a spot size of the order of 25μm for 0.543 μm light, and

64μm for 1.52μm light. The electrodes were fabricated on both -z and + z faces and were of dimensions ~12mm x 2mm and were positioned across the domain interface region. The input and output faces were parallel polished and insulating supports were used to mount the device.

4. Modelling of switching behaviour

We have developed a 2-dimensional theoretical model for the TIR switch, which can be used to predict the switching characteristics expected for any combinations of incident angle(θ_{inc}), wavelength (λ), spot size (ω_0), sample thickness (d) and wavelength dependent refractive index (n_e), as determined by the normal Sellmeier equations for $LiNbO_3$ [5].

Firstly, the model has been used to characterise the beam incident on the interface for any value of angle, θ_{inc}. In fig 4a we show a schematic for the interaction of the incident beam at the interface region. For the purposes of this model the beam incident along the interface is divided into a number of slices. The lower part of the diagram shows the corresponding intensity profile; it was found that a high a level of accuracy could be achieved by using a minimum of fifty slices. Fig 4b depicts the modelling results showing the extent to which the $1/e^2$ beam contour spreads at the interface due to the grazing angle of incidence and yields the values for where the $1/e^2$ beam profile crosses the interface. Making the assumption that the beam profile at the interface is Gaussian, the intensity profile, I, of the beam across the interface can be given for any angle of θ_{inc} using the expression

$$I = \frac{P_{total}}{l}\sqrt{\frac{2}{\pi}}\exp\left(-\frac{2z^2}{l^2}\right) \tag{3}$$

where P_{total} is the total input power of the incident beam, l is the $1/e^2$ width of the Gaussian intensity profile projected along the interface and z is the distance along the device where z=0 corresponds to the position of the beam waist. The power in each slice is given by the expression

$$P_{slice} = \frac{P_{total}}{2}\left(erf\left(\frac{\sqrt{2}x_2}{l}\right) - erf\left(\frac{\sqrt{2}x_1}{l}\right)\right) \tag{4}$$

where *erf* is the error function and x_1 and x_2 are two points that define the slice width.

There is a variation in the angle of incidence across the beam width, and this is shown in figure 5. Each slice therefore has a different effective angle of incidence, and knowing this the reflectivities of each slice can be calculated by modifying the standard Fresnel equation as applicable to fig 6 [6] to be in terms of θ_{inc} only, which becomes

$$R_s = \left(\frac{\left[\cos\left(\sin^{-1}\left[n_{it}\sin\theta_{inc} - \cos\theta_{inc}n_{it}\right]\right)\right]}{\left[\cos\left(\sin^{-1}\left[n_{it}\sin\theta_{inc} + \cos\theta_{inc}n_{it}\right]\right)\right]}\right)^2 \tag{5}$$

where $n_{it} = n_{inc}/n_t$.

The power reflected for each slice is then calculated by multiplying the reflectivity for each slice by the power in each slice. The sum of the power of the slices that have reflectivities that fall within the parameters necessary for TIR is then calculated. This

procedure is evaluated for 1000 points between 0 and 1000 Volts. The percentage of the total power is then plotted against voltage, and this allows a comparison to be made with the experimental data collected.

5. Experimental results

Fig 7 shows the geometry of interaction for the beam with the interface for all the results that follow. The $2\theta_{ext}$ angle is determined before measuring any power reflectivities and θ_{inc} is given by the expression below

$$\theta_{inc} = 90 - \theta_{int} = 90 - \left(\sin^{-1} \left(\frac{\sin\theta_{ext}}{n_e} \right) \right) \tag{6}$$

Initially results were taken using the 0.543μm laser to characterise the presence and the strength of any residual refractive index at the interface. Powers in the reflected beam were measured at various angles with no voltage applied. The data was then superimposed onto standard Fresnel reflectivity curves and visually best-fitted to obtain values for Δn in the interface region. The values of residual refractive index for both polarisations on each side of the interface can be seen in table 2.

Switching data was recorded using this wavelength for both s- and p-polarised light, and these results are shown in fig 8. As expected when considering the values of the respective electro-optic coefficients accessed by each polarisation orientation, the switching of s-polarised light occurs much before that of the p-polarised light. The contrast ratio achieved was observed to be greater than 100:1 (20dB).

Switching data was also recorded at the longer He-Ne laser wavelength of 1.52μm where good switching characteristics where again observed. Detailed comparison is now possible between the theoretical curves generated by the model, and

experimental data points. As seen in fig 9 good agreement can be obtained for the early stages of switching at low applied voltages. The lack of fit as TIR is approached can be accounted for, for example by introducing a small random angle varying between 0 and 0.2° across the interface in the numerical model to closer match the actual randomness observed for the interface. The model is now seen to round off slightly at the top, and under suitable model parameters a closer match can be obtained to the experimental results. The contrast ratio in this case for 1.52μm light is much greater than 100:1 but the measurement of exact values are currently limited by the resolution of the apparatus used for measurement.

As previously mentioned the switch is much less wavelength dependent than other electrooptic switches such as a Pockels cell, and a comparison of voltages required for TIR for the switch and the half wave voltage, V_π , for a Pockels cell confirms this. The half wave voltage for a Pockels cell can be calculated using the expression below

$$V_\pi = \frac{\lambda}{2n_e^3 r_{33}} \tag{7}$$

where λ is the wavelength of interaction. For the TIR switch, substituting for $E_z = V/d$ where V is the voltage applied across the interface and d is the switch thickness and rearranging (2) the voltage required for TIR switching can be given by the expression

$$V = \frac{2\Delta n d}{r_{33} n_e^3} = \frac{\Delta n * d}{r_{33} n_e^3} \tag{8}$$

It is clear from (7) that the value of V_π is directly proportional to λ., in contrast to our TIR switch however, in which λ does not appear. As r_{33} and n_e and their intrinsic wavelength dispersion are common to both (7) and (8) this leads to the approximation that the TIR switch operation is effectively wavelength independent. For longer wavelength operation, there are clearly geometrical factors such as Gaussian beam focussing constraints, interface lengths required and so on, but the argument concerning effective wavelength independence is valid.

6. Further work

Alternative manufacturing techniques will also be investigated; these include direct bonding of two z-cut samples of $LiNbO_3$ to form a switch consisting of two oppositely oriented domains. An advantages of this bonding technique is that no residual strain should remain as observed for the poled domain switch, and the straightness of the interface between the two domains should improve dramatically thereby. Another method of switch manufacture we are keen to investigate involves the poling technique as previously described but using *stoichiometric* lithium tantalate ($LiTaO_3$) and $LiNbO_3$. This interest has arisen because manufacturers [7] report that these crystals require a lower coercive field for poling, and have higher electro-optic coefficients than the congruent materials; the coefficients for these new materials are shown in table 3. Additionally the quality of poled interfaces has been observed to be superior to those from congruent $LiNbO_3$ [8].

7. Conclusions

We have presented a novel electro-optic switching technique that shows good contrast ratios of greater than 100:1 (20dB), by optimising the manufacturing method the contrast ratio could increase significantly and fulfil the potential associated with TIR (TIR is a 100% efficient process). The switch has been shown to function well at wavelengths of 0.543μm and the useful telecoms wavelength of 1.52μm. It has also been shown that the switching behaviour fits well to curves as predicted by a theoretical model.

8. Acknowledgements

The authors are grateful to the Engineering and Physical Sciences Research Council (EPSRC) for funding for AJB and JMH and for research funding via grant no. GR/N00302.

9. References

1. A J Boyland, G W Ross, S Mailis, P G R Smith, R W Eason, 'Total internal reflection switching in electro-optically addressable domain-engineered $LiNbO_3$', Electronics Letters, 37(9), p585-7 (2001).

2. J Li, H C Cheng, M J Kawas, D N Lambeth, T E Schlesinger, D D Stancil, 'Electro-optic wafer beam deflector in $LiTaO_3$', IEEE Photonics Technol. Lett., 8, p1486-1488, (1996)

3. R W Eason, A J Boyland, S Mailis, P G R Smith, 'Electro-optically controlled beam deflection for grazing incidence geometry on a domain-engineered interface in $LiNbO_3$', Opt. Comm, submitted April 2000.

4. R S Weis, T K Gaylord, 'Lithium niobate: Summary of Physical Properties and Crystal Structure' Applied Physics A, 37(191), p191-203(1985).

5. 'Properties of Lithium Niobate', EMIS Data Review Series No. 5, INSPEC(London), (1989)

6. E. Hecht ' Optics' Addison-Wesley, (1998)

7. Oxide Corporation datasheet. http://www.opt-oxide.com/

8. K. Kitamura, NIRIM, Japan (private communication)

Table captions

Table 1 – Examples of Δn produced and TIR angle implied for 300μm thick sample as a function of applied voltage

Table 2 – Best-fitted residual refractive index on either side of the domain boundary

Table 3 – Electro-optic coefficients and coercive fields required for domain switching for s*toichiometric* lithium tantalate and lithium niobate

Figure Captions

Fig 1 – Critical angle required for TIR as a function of voltage applied across the device of thickness 300μm

Fig 2 – Schematic diagram for domain-engineered sample

Fig 3 –Domain boundary as viewed using a polarising light microscope

Fig 4a – Schematic for interaction of incident beam with interface with the intensity profile of beam projected along the domain boundary for 1.52 μm light with a spot size of 64 μm incident at an angle of 89° where the intensity has been normalised such that total power under curve is equal to total power in beam

Fig 4b – Beam profile observed at the domain boundary for 0.543 μm light with a spot size of 25 μm incident at an angle of 89°

Fig 5 – Variation of incident beam angle across domain boundary for 1.52 μm light with a spot size of 64 μm incident at an angle of 89°

Fig 6 – Schematic for Fresnel reflection at interface

Fig 7 – Geometry of interaction

Fig 8 – Comparison of switching for s- and p- polarisations for light of 0.543 μm incident at an angle of 88.5°

Fig 9 – Comparison of model and switching data for s-polarised light at 1.52μm incident at an angle of 89.1° (points are experimental measurements, solid line is theoretical fit)

Table 1

Applied Voltage(V)	E(Vm^{-1})	Δn^*	θ_{tir}(°)
10	3.33×10^{4}	1.14×10^{-5}	89.82
100	3.33×10^{5}	1.14×10^{-4}	89.42
1000	3.33×10^{6}	1.14×10^{-3}	88.16

Table 2

	'+' side	**'-' side**
s-polarisation	1.000046	0.999890
p-polarisation	1.000020	0.999985

Table 3

Properties	**Stoichiometric $LiNbO_3$**	**Stoichiometric $LiTaO_3$**
E-field for domain switch (coercive field) (kV/mm)	< 4	< 1.7
r_{33} electrooptic coefficients (pm/V)	38.3	35.5

Figure 1

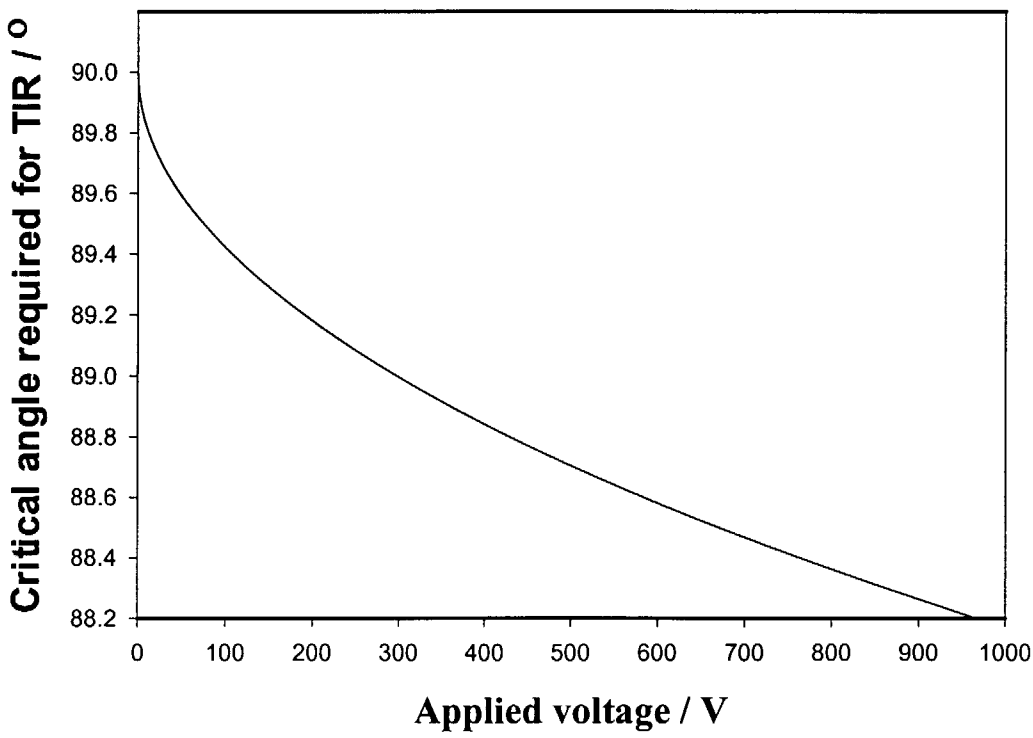
Critical angle required for TIR / °
90.0
89.8
89.6
89.4
89.2
89.0
88.8
88.6
88.4
88.2
0
100
200
300
400
500
600
700
800
900
1000
Applied voltage / V

Figure 2

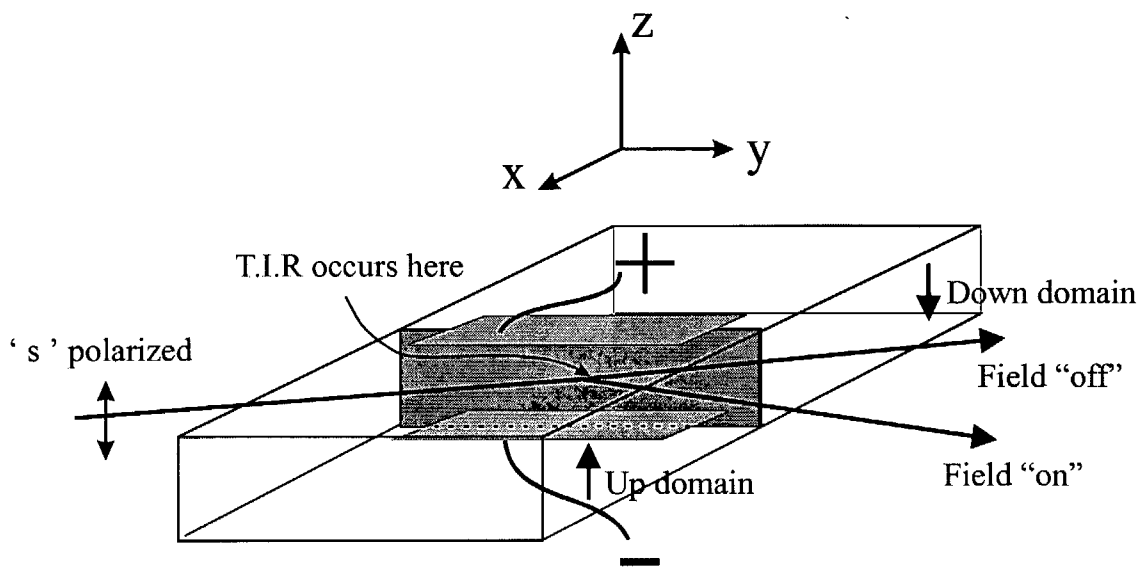
z
x
y
T.I.R occurs here
+
Down domain
' s ' polarized
Field "off"
Field "on"
Up domain
−

Figure 3

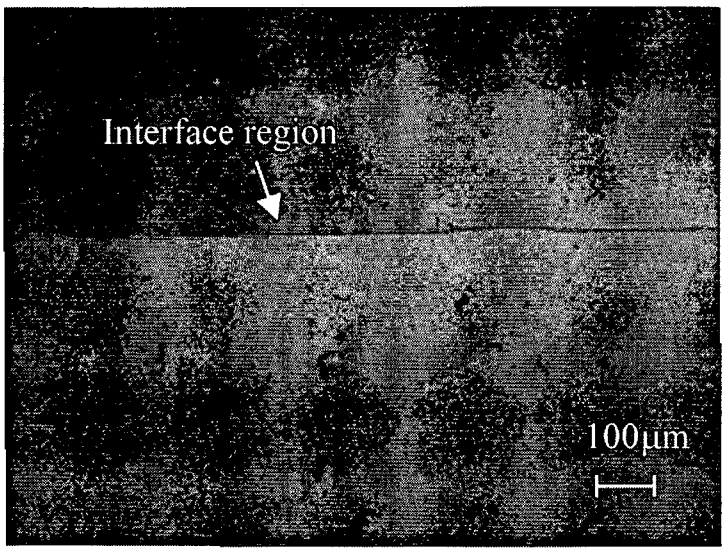

Figure 4a

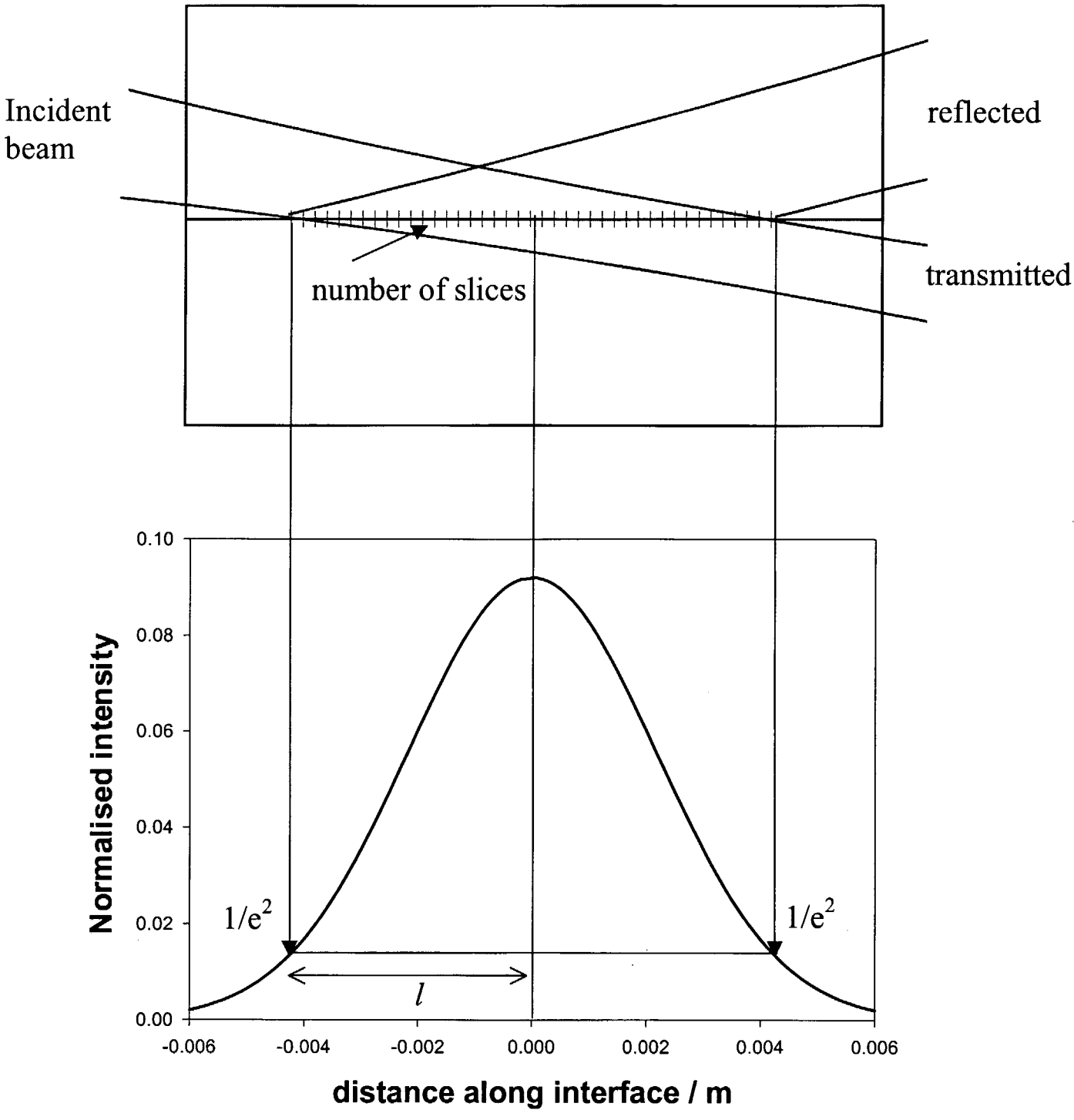
Incident beam
reflected
transmitted
number of slices
0.10
0.08
0.06
0.04
0.02
0.00
Normalised intensity
1/e2
1/e2
l
-0.006
-0.004
-0.002
0.000
0.002
0.004
0.006
distance along interface / m

Figure 4b

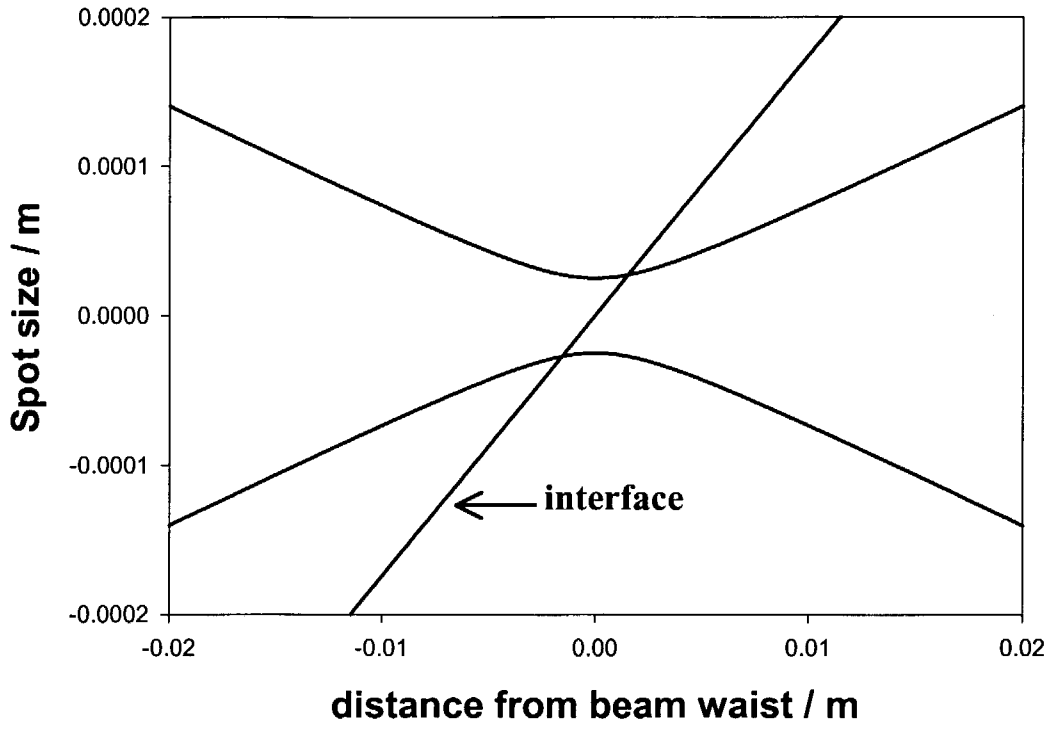
0.0002
0.0001
0.0000
-0.0001
-0.0002
Spot size / m
interface
-0.02
-0.01
0.00
0.01
0.02
distance from beam waist / m

Figure 5

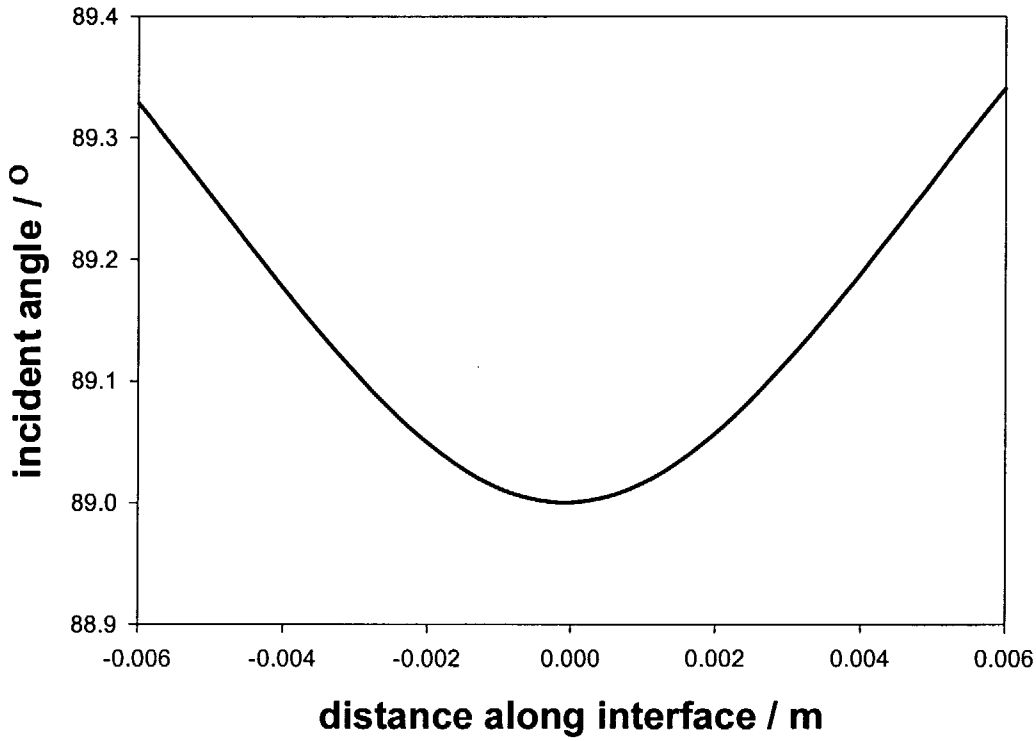
89.4
89.3
89.2
89.1
89.0
88.9
incident angle / o
-0.006
-0.004
-0.002
0.000
0.002
0.004
0.006
distance along interface / m

Figure 6

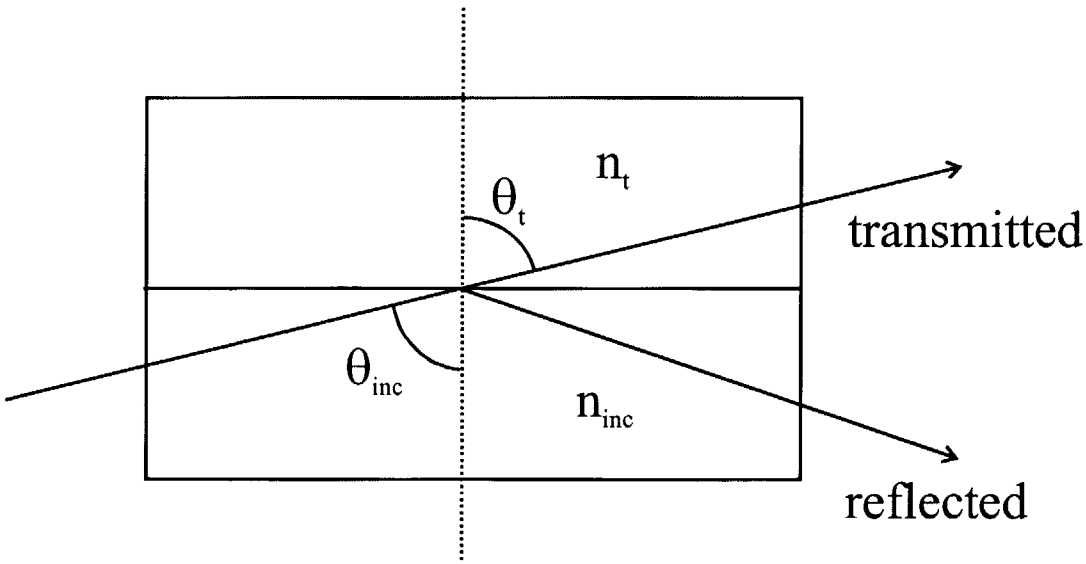

Figure 7

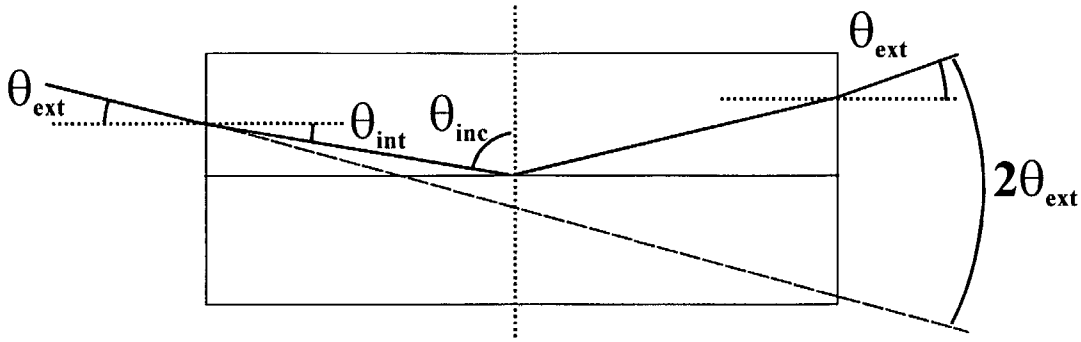

Figure 8

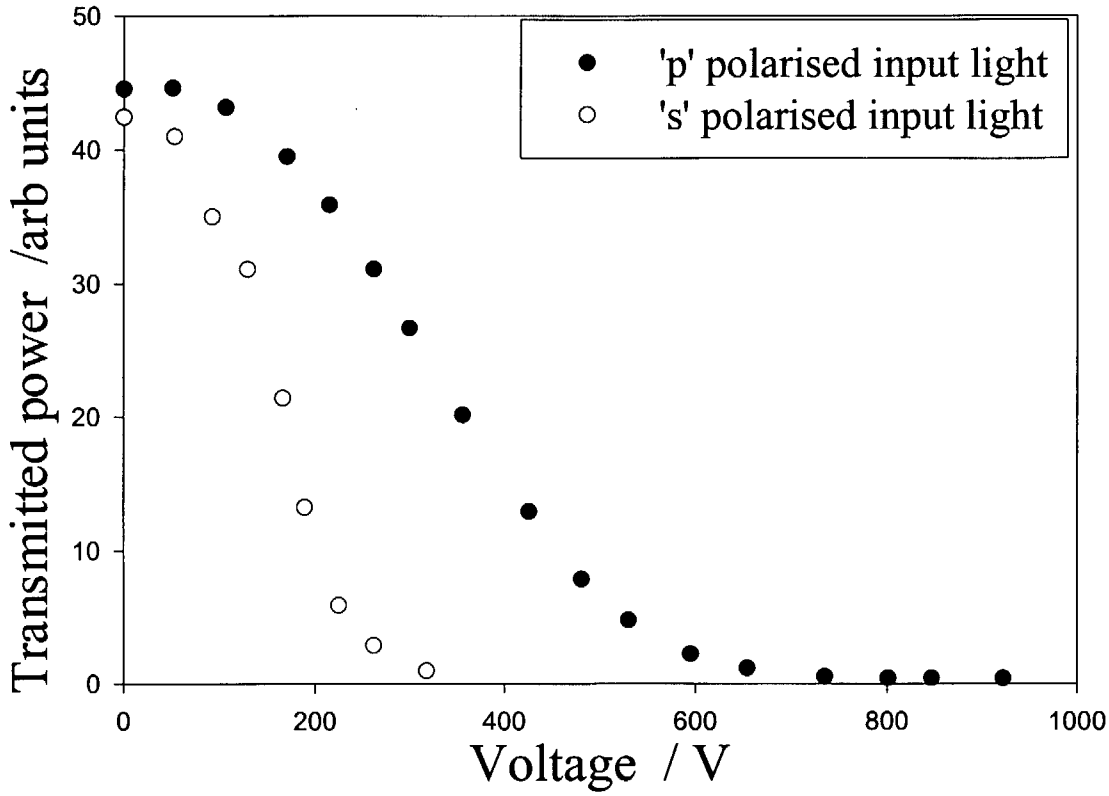
'p' polarised input light
's' polarised input light
Transmitted power /arb units
Voltage / V
0
10
20
30
40
50
0
200
400
600
800
1000

Figure 9

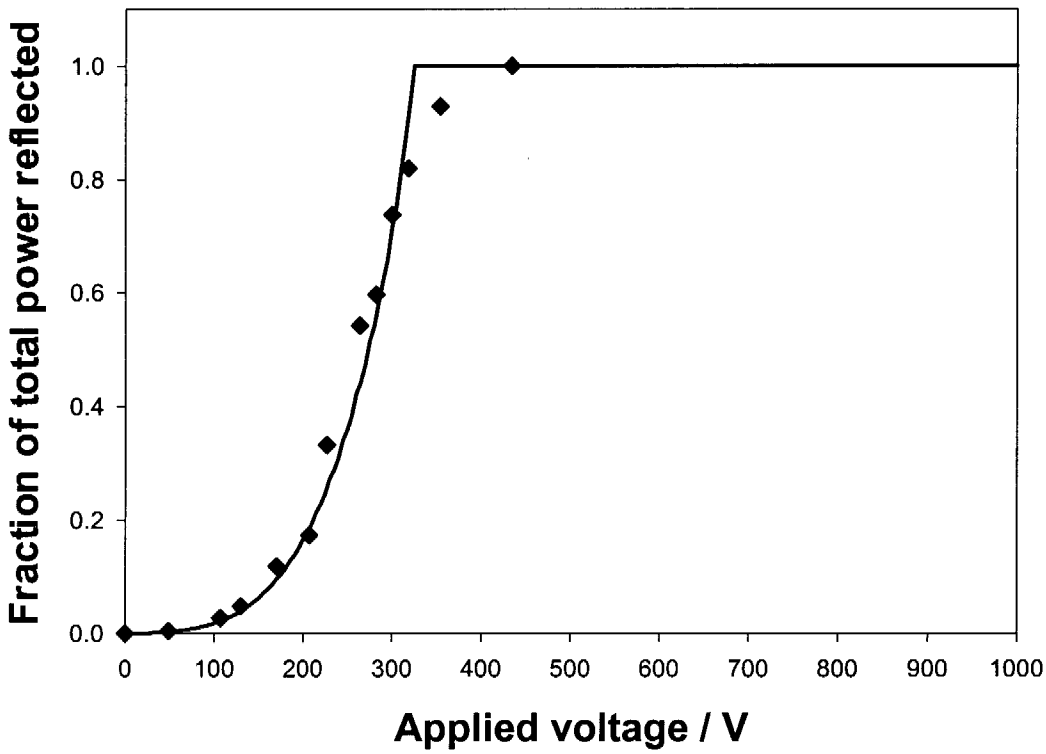
Fraction of total power reflected
1.0
0.8
0.6
0.4
0.2
0.0
0
100
200
300
400
500
600
700
800
900
1000
Applied voltage / V